PROCEEDINGS A

royalsocietypublishing.org/journal/rspa

Research

Cite this article: Bronars A, O'Reilly OM. 2019 Gliding motions of a rigid body: the curious dynamics of Littlewood's rolling hoop. *Proc. R. Soc. A* **475**: 20190440.
http://dx.doi.org/10.1098/rspa.2019.0440

Received: 16 July 2019
Accepted: 2 October 2019

Subject Areas:
mechanics, mathematical physics, differential equations

Keywords:
self-induced jumping, stick–slip phenomena, rolling rigid bodies

Author for correspondence:
Oliver M. O'Reilly
e-mail: oreilly@berkeley.edu

Electronic supplementary material is available online at https://doi.org/10.6084/m9.figshare.c.4711445.

THE ROYAL SOCIETY PUBLISHING

Gliding motions of a rigid body: the curious dynamics of Littlewood's rolling hoop

Antonia Bronars and Oliver M. O'Reilly

Department of Mechanical Engineering, University of California at Berkeley, Berkeley, CA 94720-1740, USA

OMO, 0000-0003-3773-4967

The celebrated mathematician John E. Littlewood noted that a hoop with an attached mass rolling on a ground plane may exhibit self-induced jumping. Subsequent works showed that his analysis was flawed and revealed paradoxical behaviour that can be resolved by incorporating the inertia of the hoop. A comprehensive analysis of this problem is presented in this paper. The analysis illuminates the regularity induced in the model of the hoop when its mass moment of inertia is incorporated, shows that the paradoxical motions of the hoop are consistent with the principles of mechanics and demonstrates the simplest example in the dynamics of rigid bodies that exhibits self-induced jumping.

1. Introduction

Studies on the dynamics of planar rolling motions and sliding motions of homogeneous cylinders, disks and spheres have played an important role in the development of the field of mechanics. The geometric centre and mass centres of these rigid bodies are coincident and it is easy to show that sliding motions on horizontal planes inevitably evolve to rolling motions at constant speed. When the centre of mass and geometric centre are distinct, non-planar motions are considered or the geometry of the lateral surface of the rigid body is asymmetric, then the motions often become complex and may include self-induced jumping motions [1–5], spin reversals [6], oscillations [7,8] and multiple transitions back and forth from rolling to sliding [9,10].

A remarkably simple example that illustrates some of the aforementioned complexities is discussed on page 37 of *Littlewood's Miscellany* [11]. Consider a rough weightless circular hoop to which a mass is attached and that is free to move on a horizontal plane. Suppose the

hoop is initially set in motion. Then, according to Littlewood [11], the hoop will lift off the ground. His explanation for the jumping, that the weight follows the path of a cycloid, is ingenious. However, he disputes this explanation by commenting that he expects the hoop to slip before the jump occurs. According to Littlewood, the hoop problem, which is not to be found in textbooks, was regularly posed to engineering students at the University of Cambridge by Herbert A. Webb (1862–1961).[1]

In the late 1990s, Littlewood's hoop attracted the attention of Tokieda [12] who was the first to point out that gliding motions of the hoop would occur. Gliding motions are defined as motions where the normal force (and consequently the friction force) on the hoop vanishes. Tokieda also noted that experimental evidence for jumping motions were realizable using a hula-hoop with a battery inserted into the hoop to mimic the mass particle.[2] However, Tokiedo analysis was incomplete. In response, works by Butler [16] and Pritchett [13] showed that jumping was not possible and including the inertia of the hoop might enable an explanation for the jumping motions of the hoop observed in practice. Subsequently, analysis by Theron & du Plessis [17] explained the gliding motions discussed by Tokieda [12] and numerical works by Lubarda [18], Theron & Maritz [19] and Yanzhu & Yun [20] showed a wide range of rolling, sliding and jumping (hopping) motions of a hoop with an added mass when the inertia of the hoop was considered. All of these works complement earlier independent work by Ivanov [21,22] who discovered periodic motions of a heavy cylinder with an attached mass. The motions he discovered consist of a sequence of rolling motions, jumps and impacts.

The dynamics of the weightless circular hoop with an attached mass (which we refer to as Littlewood's hoop) are paradoxical. The paradox has been partially resolved by an analysis where the inertia of the hoop is included. However, despite the large number of papers on the topic, the precise manner by which the added inertia of the hoop regularizes the problem is not clear. Our analysis reveals a vastly different dynamical system when the inertia of the hoop is included in the model. We are able to demonstrate that the rigid body consisting of a heavy circular hoop and an attached mass can roll in perpetuity, exhibit multiple transitions between rolling and sliding, and, after a transition to sliding, may even jump. When the inertia is ignored, we are easily able to show that the hoop will initially roll but will quickly lose traction. However, because the inertia of the hoop is ignored, the normal force (and the friction force) on the sliding body must vanish. Thus, the hoop will move over the rough ground plane without experiencing any frictional resistance to its motion. These are the gliding motions first discussed by Tokieda [12]. In other words, while vanishing of the normal force is a necessary (but not sufficient) condition for the hoop to jump, the possibility that it would simply glide seems to have escaped Littlewood.

In addition to Littlewood's book, our analysis of the circular hoop with an attached mass was inspired by a large number of recent works on the self-induced jumping of rigid bodies in motion on surfaces [1–5,9]. In relation to these works, the mechanics problem Littlewood contemplated is one of the simplest examples where spontaneous (or self-induced) jumping is likely to occur. While our work on the circular hoop synthesizes the earlier studies [12,13,15–20], we also provide new perspectives and new results on the dynamics of this system.

An outline of the paper is as follows. In §2, the equations of motion for a heavy circular object with an attached mass in motion on a rough horizontal surface are presented. Criteria for stick–slip behaviour and spontaneous (self-induced) jumping are also discussed. The results of our simulations of the system showing jumping and transitions from rolling to sliding and vice versa are discussed at the end of §2. We then turn to Littlewood's problem where the inertia of the rigid body is ignored. The equations of motion for this system are easily obtained by specializing the results for the heavy rigid body. As discussed in §3, the resulting equations of motion are integrable. With appropriate initial conditions, we find that the hoop and attached mass can roll. After a finite period of time, the rolling motion will transition to gliding, and, after a finite period

[1]We must also express our admiration for the students who answered Webb's question correctly.

[2]Other demonstrations can be found in [13–15].

of time, the attached mass will reach the horizontal ground plane. Furthermore, the path of the attached mass during the gliding phase will either be a parabolic curve or a straight line.

2. The governing equations for the rigid body

We consider the classic problem of a rigid body composed of a circular disc with a rigidly attached particle of mass m_2 (cf. figure 1) moving on a rough surface. The axisymmetric body has a mass moment of inertia I_{zz}, mass m_1 and an outer radius R. The particle of mass m_2 is located at a distance ℓ from C. Owing to the presence of the particle of mass m_2, the centre of mass $\bar{X}$ of the rigid body of mass $m = m_1 + m_2$ is no longer located at the geometric centre C of the circular disc. The moment of inertia of the rigid body of mass m relative to $\bar{X}$ is

$$I = I_{zz} + \frac{m_1 m_2}{m_1 + m_2}\ell^2. \tag{2.1}$$

Our notation and the methodology we use to develop the equations of motion for the rigid body follow [23]. We shall assume that the rotational motion of the rigid body of mass m is such that it has a fixed axis of rotation and that the body moves with a single instantaneous point of contact X_P on a rough horizontal plane. Thus, the kinematics of the rigid body can be captured by a single angle of rotation θ and a coordinate η.

We define a fixed right-handed Cartesian basis $\{\mathbf{E}_1, \mathbf{E}_2, \mathbf{E}_3 = \mathbf{E}_1 \times \mathbf{E}_2\}$ and a right-handed corotational basis $\{\mathbf{e}_1, \mathbf{e}_2, \mathbf{e}_3 = \mathbf{E}_1 \times \mathbf{E}_2\}$:

$$\mathbf{e}_1 = \cos(\theta)\,\mathbf{E}_1 + \sin(\theta)\,\mathbf{E}_2 \quad \text{and} \quad \mathbf{e}_2 = \cos(\theta)\,\mathbf{E}_2 - \sin(\theta)\,\mathbf{E}_1. \tag{2.2}$$

The position of the instantaneous point of contact X_P relative to the centre of mass $\bar{X}$ of the rigid body has the representation

$$\boldsymbol{\pi}_P = -R\mathbf{E}_2 - h\mathbf{e}_2, \tag{2.3}$$

where

$$h = \frac{m_2}{m_1 + m_2}\ell. \tag{2.4}$$

To apply the results of our analysis to the problem considered by Littlewood, we simply need to set $I_{zz} = 0$, $\ell = R$, $h = R$ and $m_1 = 0$.

The position vectors of the centre of mass and the geometric centre C of the disc have the respective representations

$$\bar{\mathbf{x}} = \bar{x}\mathbf{E}_1 + \bar{y}\mathbf{E}_2 \quad \text{and} \quad \mathbf{x} = x\mathbf{E}_1 + y\mathbf{E}_2, \tag{2.5}$$

where $\mathbf{x} = \bar{\mathbf{x}} - h\mathbf{e}_2$. When the body is in motion on the plane, y is constant. To describe the dynamics of the rigid body when it is sliding, it is convenient to define the following coordinate:

$$\eta = x + R\theta. \tag{2.6}$$

The velocity vector of the point X_P when the body is in motion on the plane has several representations:

$$\begin{aligned}\mathbf{v}_P &= \dot{\eta}\mathbf{E}_1\\ &= \left(\dot{x} + R\dot{\theta}\right)\mathbf{E}_1\\ &= \left(\dot{\bar{x}} + (R + h\cos(\theta))\,\dot{\theta}\right)\mathbf{E}_1 + \left(\dot{\bar{y}} + h\sin(\theta)\,\dot{\theta}\right)\mathbf{E}_2.\end{aligned} \tag{2.7}$$

Thus, $\dot{\eta}\mathbf{E}_1$ is the slip velocity of the rigid body. The kinetic energy T and potential energy U of the rigid body have the representations

$$\begin{aligned}T &= \frac{m}{2}\left(\dot{\bar{x}}^2 + \dot{\bar{y}}^2\right) + \frac{I}{2}\dot{\theta}^2\\ &= \frac{1}{2}\left(I + (m_1 + m_2)\left(R^2 + h^2 + 2Rh\cos(\theta)\right)\right)\dot{\theta}^2\end{aligned}$$

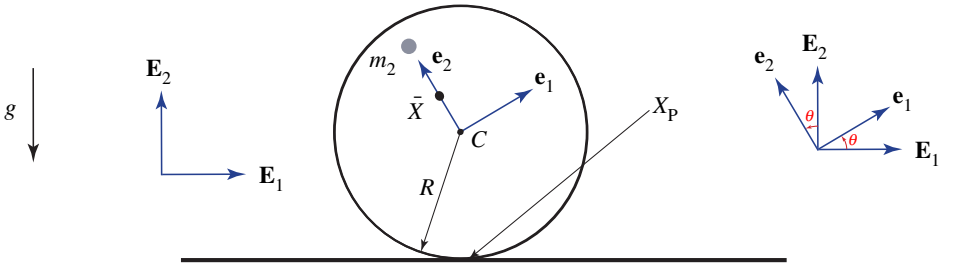

Figure 1. Schematic of a body moving on a rough horizontal surface. The point X_P is the instantaneous point of contact of the body with the ground plane. Because of the added mass m_2, the geometric centre C of the circular body is not the centre of mass $\bar{X}$ of the composite body. (Online version in colour.)

$$+\frac{m_1+m_2}{2}\left(\dot{\eta}^2-2\dot{\eta}\dot{\theta}\left(R+h\cos\left(\theta\right)\right)\right)$$

and
$$U=m_2g\ell\cos\left(\theta\right). \tag{2.8}$$

The expression for the kinetic energy of the rolling rigid body can be obtained from $(2.8)_1$ by setting the slip speed $\dot{\eta}=0$. When $I_{zz}\neq 0$, the mass matrix associated with the kinetic energies of the rolling rigid body and the sliding rigid body are always strictly positive.

In the sequel, we shall non-dimensionalize time t, the normal force N, friction forces $F_{f_{\text{static}}}$ and $F_{f_{\text{dynamic}}}$ and parameters of the systems as follows:

$$\begin{aligned}
&t\to\tau=\sqrt{\frac{g}{R}}t,\quad \eta\to\hat{\eta}=\frac{\eta}{R},\quad m_1\to\hat{m}_1=\frac{m_1}{m_2},\\
&\ell\to\hat{\ell}=\frac{\ell}{R},\quad h\to\hat{h}=\frac{h}{R}=\frac{\hat{\ell}}{1+\hat{m}_1},\quad I_{zz}\to\hat{I}_{zz}=\frac{I_{zz}}{m_2R^2},\quad I\to\hat{I}=\frac{I}{m_2R^2}=\hat{I}_{zz}+\frac{\hat{m}_1\hat{\ell}^2}{1+\hat{m}_1},\\
&N\to\hat{N}=\frac{N}{m_2g},\quad F_{f_{\text{static}}}\to\hat{F}_{f_{\text{static}}}=\frac{F_{f_{\text{static}}}}{m_2g},\quad F_{f_{\text{dynamic}}}\to\hat{F}_{f_{\text{dynamic}}}=\frac{F_{f_{\text{dynamic}}}}{m_2g}.
\end{aligned} \tag{2.9}$$

Using m_2 to non-dimensionalize the mass enables us to analyse Littlewood's problem by setting $\hat{I}=0$, $\hat{\ell}=1$ and $\hat{m}_1=0$.

(a) Equations of motion for the rolling rigid body

The resultant force $\mathbf{F}$ acting on the rolling rigid body is composed of a normal force $N\mathbf{E}_2$ and a static friction force $\mathbf{F}_f=F_{f_{\text{static}}}\mathbf{E}_1$ acting at X_P and a gravitational force $-mg\mathbf{E}_2$ acting at $\bar{X}$. The equations of motion for the rigid body are obtained from a combination of the constraint equations $\mathbf{v}_P=\mathbf{0}$, $\mathbf{F}=m\ddot{\bar{\mathbf{x}}}$ and the moment balance $I\ddot{\theta}=(\boldsymbol{\pi}_P\times(\mathbf{F}_f+\mathbf{N}))\cdot\mathbf{E}_3$. After some algebraic manipulations, the equations of motion for the rigid body of mass $m=m_1+m_2$ when the body is rolling can be expressed as the following set of equations:

$$\dot{\eta}=0\quad\text{and}\quad\ddot{\theta}=f_R\left(\theta,\dot{\theta}\right), \tag{2.10}$$

where the function

$$f_R\left(\theta,\dot{\theta}\right)=\frac{\left(m_1+m_2\right)Rh\sin\left(\theta\right)\dot{\theta}^2+m_2g\ell\sin(\theta)}{I+\left(m_1+m_2\right)\left(R^2+h^2+2Rh\cos\left(\theta\right)\right)}. \tag{2.11}$$

In addition, expressions for the normal force $\mathbf{N}=N\mathbf{E}_2$ and the static friction force $\mathbf{F}_f=F_{f_{\text{static}}}\mathbf{E}_1$ acting on the rolling rigid body can be found:

$$\begin{aligned}
N&=\left(m_1+m_2\right)g-m_2\ell\left(\sin\left(\theta\right)f_R\left(\theta,\dot{\theta}\right)+\cos\left(\theta\right)\dot{\theta}^2\right),\\
F_{f_{\text{static}}}&=-\left(m_1+m_2\right)\left(R+h\cos\left(\theta\right)\right)f_R\left(\theta,\dot{\theta}\right)+m_2\ell\sin\left(\theta\right)\dot{\theta}^2.
\end{aligned} \tag{2.12}$$

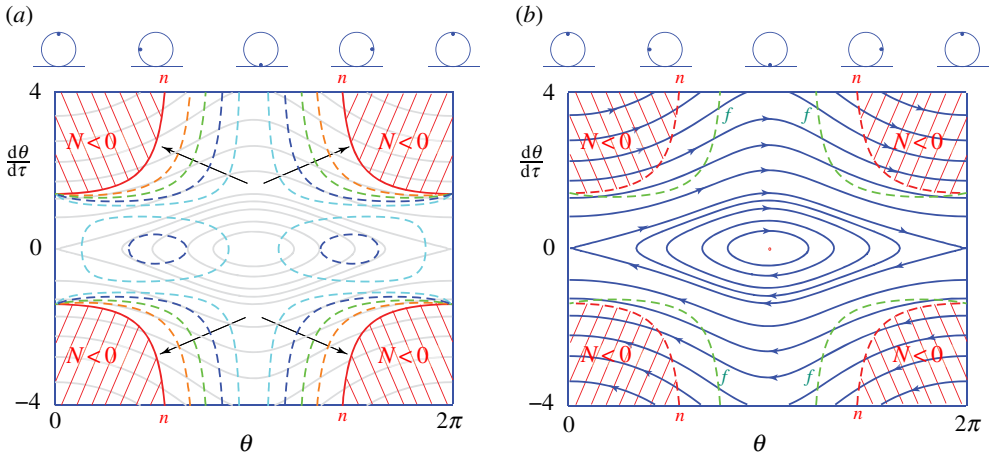

Figure 2. (*a*) The $\theta - \theta'$ plane showing the loci of points where $|F_{f_{\text{static}}}| = \mu_s N$. The curves shown correspond to $\mu_s = 0.1, 0.25, 0.5$ and 1.0. The arrows indicate the direction of increasing μ_s. As $\mu_s \to \infty$ the curve asymptotes to the locus of points (labelled *n*) where $N = 0$. Level sets of the total energy are also shown. (*b*) Phase portrait of the equations of motion (2.10) for the rolling rigid body. The curves labelled *f* correspond to the locus of points $|F_{f_{\text{static}}}| = \mu_s N$ where $\mu_s = 0.5$, and the curve labelled *n* corresponds to the locus of points where the normal force vanishes (i.e. $N = 0$). For the results shown in this figure, $(m_1/m_2) = 1$, $\ell = R$ and $I_{zz} = m_1 R^2$. (Online version in colour.)

For the rigid body to maintain contact, we require $N > 0$ and the satisfaction of the static friction criterion:

$$|F_{f_{\text{static}}}| \leq \mu_s N, \tag{2.13}$$

where μ_s is the static coefficient of friction.

The total energy $T + U$ of the rolling rigid body is conserved during a motion. With the help of the static friction criterion and the condition that $N > 0$, regions $\mathcal{N}$ and $\mathcal{R}$ of the $\theta - \theta' - \eta'$ state space can be defined:

$$\begin{aligned} \mathcal{N} &= \left\{(\theta, \theta', \eta') \,|N > 0\right\}, \\ \mathcal{R} &= \left\{(\theta, \theta', \eta') \,|\, |F_{f_{\text{static}}}| \leq \mu_s N \text{ and } N > 0\right\}. \end{aligned} \tag{2.14}$$

Here, the $'$ denotes the derivative with respect to τ: e.g. $\theta' = \mathrm{d}\theta/\mathrm{d}\tau$. If the initial conditions for the rigid body are such that they lie in $\mathcal{R}$, then the body will roll initially. As can be seen from figure 2*a*, as μ_s increases, the region $\mathcal{R}$ of the $\theta - \theta'$ plane increases in size as μ_s increases to the region $\mathcal{N}$ where $N > 0$. The hatched areas shown in figure 2*a*,*b* correspond to regions of the $\theta - \theta'$ plane where $N < 0$. The regions $\mathcal{R}$ and $\mathcal{N}$ depend on the values of $\hat{m}_1$ and $\hat{I}$, while the region $\mathcal{R}$ additionally depends on the value of μ_s.

The dynamics of the rolling rigid body are easily visualized with the help of a phase portrait of (2.10) in the $\theta - \dot{\theta}$ plane that is shown in figure 2*b*. The trajectories in this portrait correspond to level sets of the total energy of the rigid body. As anticipated, (2.10) has a pair of equilibria: an unstable equilibrium $(\theta = 0, \theta' = 0)$ where m_2 is at its highest point and a stable equilibrium $(\theta = \pi, \theta' = 0)$ where m_2 is closest to the ground plane. The set of points where the friction criterion is violated and the normal force vanishes are also shown in the figure. Clearly, it is possible to set the rigid body in motion in such a manner that N vanishes immediately.[3] The motions that are of particular interest here are those where the rigid body is rolling initially and $N > 0$. In this case, we observe from the phase portrait that the body will either slip before N vanishes or will continue

[3]For instance, if the initial conditions for the rigid body were $(\theta(\tau_0) = 0, \theta(\tau_0) = 4)$.

to roll indefinitely.[4] To explore the possibility of N vanishing or the possibility of a transition from slipping to rolling, the equations for a sliding rigid body must be examined.

(b) Equations of motion for the sliding rigid body

When the body is sliding, then the friction force is dynamic and opposes the slip velocity $\mathbf{v}_P$:

$$\mathbf{F}_f = F_{f_{\text{dynamic}}}\mathbf{E}_1 = -\mu_k N \frac{\dot{\eta}}{|\dot{\eta}|}\mathbf{E}_1. \tag{2.15}$$

The equations of motion for the sliding rigid body can be obtained from a combination of the constraint equation $\mathbf{v}_P \cdot \mathbf{E}_2 = 0$, $\mathbf{F} = m\ddot{\mathbf{x}}$, and the moment balance $I\ddot{\theta} = (\boldsymbol{\pi}_P \times (\mathbf{F}_f + \mathbf{N})) \cdot \mathbf{E}_3$. After some algebraic manipulations and reorganization, a pair of differential equations for η and θ can be found:

$$\mathtt{M}\begin{bmatrix}\ddot{\eta}\\ \ddot{\theta}\end{bmatrix} + \begin{bmatrix} mh\sin(\theta)\,\dot{\theta}^2 \\ -mRh\sin(\theta)\,\dot{\theta}^2\end{bmatrix} = \begin{bmatrix} -\mu_k\left((m_1+m_2)\,g - m_2\ell\cos(\theta)\,\dot{\theta}^2\right)\dfrac{\dot{\eta}}{|\dot{\eta}|} \\ m_2 g\ell\sin(\theta)\end{bmatrix}, \tag{2.16}$$

where

$$\mathtt{M} = \begin{bmatrix} m & -m\,(R + h\cos(\theta)) - \mu_k m_2 \ell\sin(\theta)\,\dfrac{\dot{\eta}}{|\dot{\eta}|} \\ -m\,(R + h\cos(\theta)) & I + m\left(R^2 + h^2 + 2Rh\cos(\theta)\right)\end{bmatrix}. \tag{2.17}$$

We also note that, in the absence of friction, the mass matrix $\mathtt{M}$ would be symmetric as expected. The expression for the normal force N that was used to expand and manipulate the expression for $F_{f_{\text{dynamic}}}$ in (2.16) is

$$N = (m_1 + m_2)\,g - m_2\ell\left(\sin(\theta)\,\ddot{\theta} + \cos(\theta)\,\dot{\theta}^2\right), \tag{2.18}$$

where $\theta(t)$ satisfies (2.16). We emphasize that the equations of motion assume that $N > 0$. The motion of the sliding rigid body dissipates the total energy. In addition, the dynamics in this case can be visualized by examining the orbits of (2.16) in the $\theta - \dot{\theta} - \dot{\eta}$ space.

(c) Stick–slip transitions

Stick–slip transitions for the rigid body occur when there is insufficient static friction to maintain rolling (i.e. the static friction criterion is violated). In this case, the motion of the disc is no longer governed by (2.10) but instead by (2.16). The sign of F_{static} at the instant of slip is used to determine the initial slip direction. Simulation of the motion using (2.16) proceeds until $\dot{\eta}$ drops below a threshold ($\approx 10^{-9}$) and the simulations are then performed using (2.10).

(d) Spontaneous jumping

For spontaneous jumping of the rigid body to occur at the instant, it is necessary that the normal force N vanishes. The expressions $(2.12)_1$ and (2.18) for the rolling and sliding cases, respectively, are used to determine the instances when jumping occurs. A sufficient condition for jumping to occur when N vanishes is that the vertical velocity $\dot{\tilde{y}}$ of the centre of mass is strictly positive. When the body is in motion on the horizontal plane, we have that $\dot{\tilde{y}} = -h\sin(\theta)\dot{\theta}$ and $\dot{\tilde{x}} = \dot{\eta} - (R + h\cos(\theta))\dot{\theta}$. Thus, the quadrants in the $\theta - \dot{\theta}$ plane where $\sin(\theta)\dot{\theta} < 0$ are the possible locations of the spontaneous jumping.[5] From the expression for $\dot{\tilde{x}}$, we observe that if the body loses contact while rolling to the right (i.e. $\dot{\theta} < 0$), then the jump will be to the right (i.e. $\dot{\tilde{x}} > 0$) and vice versa.

[4] A video showing a simulation of a rolling motion that oscillates back and forth about the stable equilibrium configuration is given in the electronic supplementary material for this paper.

[5] Our results here extend those that of Yanzhu & Yun [20].

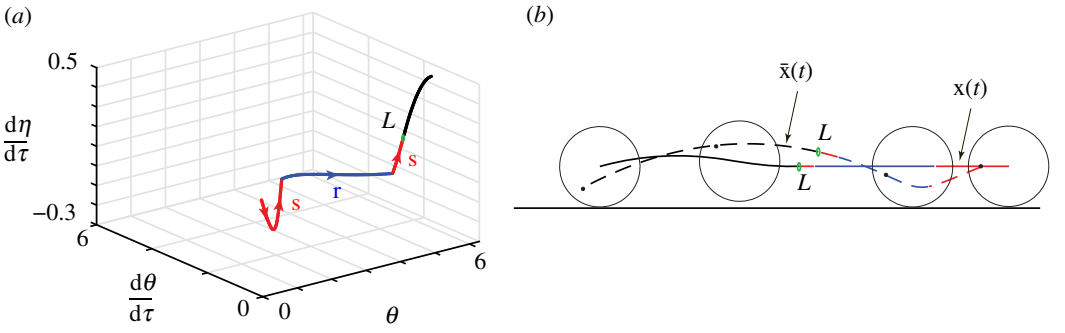

Figure 3. Representation of the motion of a rigid body that slides, rolls, slides and then jumps. (*a*) State space representation for the sliding (labelled s) and rolling phases (labelled r) before the lift-off (labelled *L*) occurs. (*b*) The loci x(*t*) of the geometric centre and $\bar{\mathrm{x}}(t)$ of the mass centre $\bar{X}$ of the rigid body during the sliding, rolling, sliding and airborne stages of the motion. For the results shown in this figure, $(m_1/m_2) = 1$, $\ell = R$, $I_{zz} = m_1R^2$, $\mu_s = 0.5$, $\mu_k = 0.4$, $\theta(0) = (\pi/2)$, $\theta'(0) = 2$ and $\eta'(0) = 0$. An animation of the results shown in (*b*) can be found in the electronic supplementary material. (Online version in colour.)

(e) Free-flight and impact

While the body is in motion on the plane, $y = R$. Once the body was launched, the sole force acting on the body is gravity and the angular velocity of the body is constant. Thus, the path of the centre of mass $\bar{X}$ will be a parabola and the geometric centre C will rotate about $\bar{X}$ at a constant rate. Once, the height y of C, declines to a value of R, then the rigid body will impact with the surface. In our work, we limit our analysis to the instant just before the impact and do not consider the post-impact dynamics of the rigid body.[6]

(f) A representative example

A representative example of a motion of the rigid body that has a slip–stick transition followed by a stick–slip transition before an eventual free-flight stage is shown in figure 3. The initial conditions for the motion of the rigid body are $(\theta(0) = (\pi/2), \theta'(0) = 2, \eta' = 0)$ and $\mu_s = 0.5$. As can be seen from figure 2*b*, for this set of initial conditions, there is insufficient static friction to maintain rolling and the rigid body slides. A transition to rolling and back to sliding occurs before the body loses contact with the ground plane. As anticipated from our earlier discussion, the jump in the motion of the centre of mass is to the left and during the free-flight stage, the path of the centre of mass is parabolic.

Related examples where the body has a single stick–slip transition before jumping and a single sliding phase before jumping were also found. In the interests of brevity, they are not presented here. We also emphasize that it is possible to give the body a set of initial conditions so that rolling persists for all time. Similarly, it is possible for the body to have phases of rolling motions and sliding motions without ever jumping off the ground plane. Closely related numerical studies of the behaviour of the rigid body can be found in Lubarda [18] and Theron and Maritz [19]. The qualitative discussion of the dynamics of the rigid body presented with its accompanying phase portrait that is presented in this section complements these works by providing another perspective on their simulations.

3. Littlewood's problem

On page 37 of *Littlewood's Miscellany* [11], one finds the following problem: 'A weight is attached to a point of a rough weightless hoop, which then rolls in a vertical plane, starting near the position

[6]Readers interested in the impact dynamics are referred to Ivanov [2,21,22].

of unstable equilibrium. What happens, and is it intuitive?' Littlewood continues, 'The hoop lifts off the ground when the radius vector to the weight becomes horizontal. I don't find the lift directly intuitive; one can, however, "see" that the motion is equivalent to the weight's sliding smoothly under gravity on the cycloid that it describes, and it is intuitive that it will sooner or later leave *that*.' He concludes with the remark: 'In actual practice the hoop skids first.'

The case considered by Littlewood assumes that $\hat{I}=0$, $\ell=R$ and $m_1=0$.[7] In our analysis, we first consider the rolling case and then consider the sliding case. Our conclusions differ significantly from Littlewood's. First, we find that the hoop cannot lift off the ground when $\theta=\pm(\pi/2)$. Second, because the inertia of the hoop is ignored, we are able to show in two ways that the rigid body cannot support a normal force and so the body glides rather than slides. Finally, based on our earlier results in the present paper, the jumping motions Littlewood describes can only occur if the inertia of the hoop is considered and they do not necessarily occur when $\theta=\pm(\pi/2)$.

The most comprehensive treatment of Littlewood's hoop in the literature to date is by Theron & du Plessis [17]. These authors corrected errors in the earlier works [12,13,16]. In this work, we are able to provide a different qualitative perspective on their analytical results. Our work also clearly illuminates the singular behaviour of Littlewood's hoop compared to the rigid body where the inertia of the hoop is considered. We also provide a clearer interpretation of how the balance laws provide a system of determinate equations to determine the motion of Littlewood's hoop compared to [17].

(a) Rolling motions

When $\hat{I}=0$, $\ell=R$ and $m_1=0$, the equations of motion (2.10) for the rolling rigid body simplify to

$$2\left(1+\cos\left(\theta\right)\right)\theta''=\left(1+\theta'\theta'\right)\sin\left(\theta\right). \tag{3.1}$$

Observe that the differential equation is identically satisfied by $(\theta(\tau)=\pi,\dot{\theta}(\tau))$ (i.e. the particle of mass m_2 is in contact with the ground) and has an equilibrium when $(\theta(\tau)=0,\dot{\theta}(\tau)=0)$ (i.e. the particle of mass m_2 is a distance $2R$ directly above the point X_{P} of contact). In contrast to the case where $I_{zz}\neq 0$, the mass matrix associated with the kinetic energy is singular when $\theta=\pi$. For the rolling rigid body, the configuration manifold is a circle and the coordinate θ fails to parametrize the entire circle.[8] The presence of the singularity also implies that the equations of motion do not accommodate the case where the particle of mass m_2 is in contact with the ground. The phase portrait of (3.1) is shown in figure 4. Qualitatively, there are dramatic differences between the trajectories in this portrait compared to those shown in the phase portrait when $m_1\neq 0$ shown in figure 2*b*. In particular, the stable equilibrium at $\theta=\pm\pi$ found earlier when $m_1\neq 0$ has vanished.

The equations of motion (3.1) have a first integral corresponding to the dimensionless total energy of the rigid body:

$$e=\frac{T+U}{m_2gR}=\left(1+\cos\left(\theta\right)\right)\theta'\theta'+\cos\left(\theta\right). \tag{3.2}$$

This conservation of energy enables us to solve for $\theta(\tau)$ using a standard procedure:

$$\sin\left(\frac{\theta\left(\tau\right)}{2}\right)=\frac{\alpha}{2}\mathrm{e}^{\left(\left(\tau-\tau_0/2\right)\right)}-\frac{e_0-1}{4\alpha}\mathrm{e}^{\left(-\left(\tau-\tau_0/2\right)\right)}. \tag{3.3}$$

[7]We can also relax the assumption that $\ell=R$ and assume that the mass particle does not lie next to the rim of the circular body. The results for this case are qualitatively similar to those for $\ell=R$ and little is gained by adding this additional feature to the model.

[8]Our perspective on coordinate singularities is based on the recent work [24].

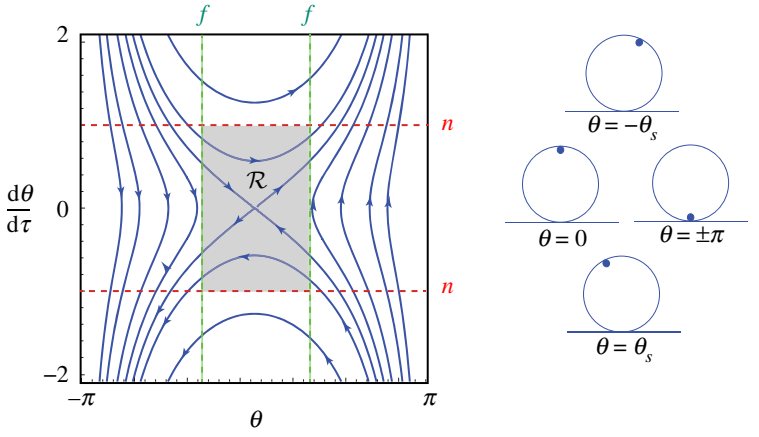

Figure 4. Phase portrait of the equations of motion (3.1) for the rolling rigid body. The shaded region corresponds to the states $(\theta, \theta', \eta') \in \mathcal{R}$ where the normal force is positive and the static friction criterion is satisfied. The region $\mathcal{R}$ shrinks to zero as $\mu_s \to 0$. The curves labelled *f* correspond to the locus of points where the static friction criterion is violated (i.e. $|F_{f_{\text{static}}}| = \mu_s N$) and the curve labelled *n* corresponds to the locus of points where the normal force vanishes (i.e. $N = 0$). For the results shown in this figure, $\mu_s = 0.5$. (Online version in colour.)

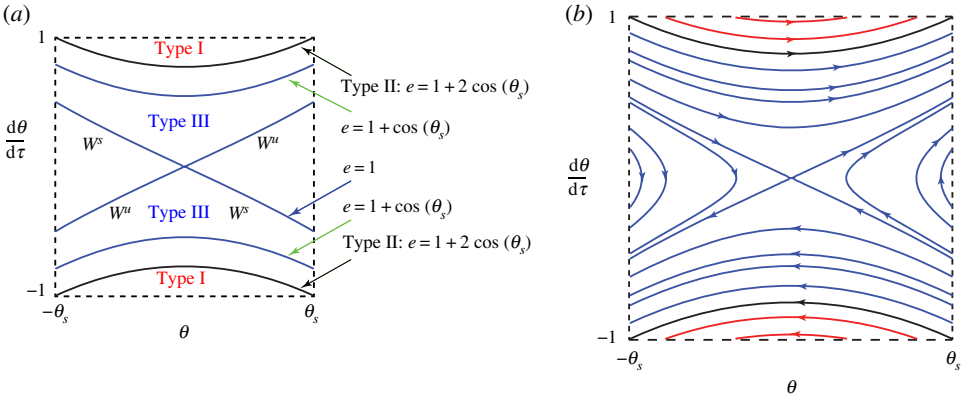

Figure 5. (*a*) The region $\mathcal{R}$ of the phase portrait of (3.1) showing the labels of the regions and boundaries where $N > 0$ and the static friction criterion is satisfied. (*b*) The phase portrait of the equations of motion (3.1) for the rolling rigid body. Motions of the rigid body where *N* vanishes before slipping correspond to solutions labelled Type I and motions that slip before *N* vanishes are classified as Type III. When $\theta_s' = \pm 1$, $N = 0$ and when $\theta = \pm\theta_s$, $F_f = \pm\mu_s N$. For the results shown in this figure, $\mu_s = 0.5$ and $\theta_s = 26.5651^\circ$. (Online version in colour.)

The constants e_0 and α are determined by the initial conditions:

$$e_0 = (1 + \cos(\theta(\tau_0)))\,\theta'(\tau_0)\,\theta'(\tau_0) + \cos(\theta(\tau_0)),$$
$$\alpha = \sin\left(\frac{\theta(\tau_0)}{2}\right) + \frac{1}{\sqrt{2}}\sqrt{e_0 - \cos(\theta(\tau_0))}. \tag{3.4}$$

Suppose the initial conditions of interest are such that neither $\theta(\tau_0) \neq \pi$ nor the initial conditions $(\theta(\tau_0), \theta'(\tau_0))$ lie on the stable W^s manifold (or separatrices) of the equilibrium $(\theta, \theta') = (0, 0)$ (cf. figure 5*a*).In this case, we now demonstrate using (3.3) that $\sin((\theta(\tau)/2)) \to \pm 1$ in a finite time. The first set of solutions to see this behaviour are motions with the initial conditions $(\theta(\tau_0) = \theta_0, \theta'(\tau_0) = 0)$. For this pair of initial conditions, $e_0 = \cos(\theta_0)$ and (3.3) simplifies to

$$\sin\left(\frac{\theta(\tau)}{2}\right) = \sin\left(\frac{\theta_0}{2}\right)\text{Cosh}\left(\frac{\tau - \tau_0}{2}\right). \tag{3.5}$$

Thus, $\theta(\tau) \to \pi$ in a finite interval of $\tau - \tau_0$. The second case to consider are solutions with initial conditions $(\theta(\tau_0) = 0, \theta'(\tau_0) = \theta_0')$. In this instance, it is straightforward to show that

$$\sin\left(\frac{\theta(\tau)}{2}\right) = \theta_0' \,\mathrm{Sinh}\left(\frac{\tau - \tau_0}{2}\right), \tag{3.6}$$

and, thus, $\theta(\tau) \to \pi$ in a finite interval of time. For completeness, we consider the case where the initial conditions lie on the stable W^s and unstable W^u manifolds of the equilibrium point $(\theta, \theta') = (0, 0)$. For these initial conditions, $e_0 = 1$, and (3.3) can be used to show that

$$\sin\left(\frac{\theta(\tau)}{2}\right) = \sin\left(\frac{\theta_0}{2}\right) \mathrm{e}^{(\pm(\tau - \tau_0/2))}, \tag{3.7}$$

where the $-$ and $+$ cases pertain to initial conditions on W^s and W^u, respectively. In conclusion, apart from motions whose initial conditions lie on the stable manifold W^s of the equilibrium $(\theta, \theta') = (0, 0)$, the solutions to (3.1) imply that the rigid body will roll in such a manner that $\theta \to \pi$ in a finite time.

Our conclusions about the behaviour to the solutions to (3.1) have ignored consideration of the normal force and friction force. The expressions for the dimensionless normal force and friction force can be obtained from (2.12):[9]

$$\begin{aligned} \hat{N} &= \cos^2\left(\frac{\theta}{2}\right)(1 - \theta'\theta'), \\ \hat{F}_{f_{\text{static}}} &= (\theta'\theta' - 1)\cos\left(\frac{\theta}{2}\right)\sin\left(\frac{\theta}{2}\right). \end{aligned} \tag{3.8}$$

Thus, for contact, we require that $|\theta'| < 1$. The locus of points where the static friction criterion is violated is given by the values of $\theta = \theta_s$ which satisfy

$$\mu_s = \left|\tan\left(\frac{\theta_s}{2}\right)\right|. \tag{3.9}$$

The region $\mathcal{R}$ of the $\theta - \theta' - \eta'$ state space for this problem is easily constructed:

$$\mathcal{R} = \left\{(\theta, \theta', \eta') \,|\theta \in (-\theta_s, \theta_s)\,,\ \theta' \in (-1, 1)\,,\ \text{and}\ \eta' = 0\right\}. \tag{3.10}$$

This region is shown in figure 5.

Based on the results of our forthcoming analyses, it is convenient to categorize motions of the rigid body into three types. Referring to figure 5*a*, Type I are motions where N vanishes before the static friction criterion has been violated, Type II are motions where N vanishes just as the static friction criterion is invalidated and Type III are motions that eventually leading to slipping with $N > 0$. With the help of the definition of θ_s and e, the motions of the rigid body can be classified to terms of e and μ_s:

Type I: $1 + 2\cos(\theta_s) < e < 3$;
Type II: $e = 1 + 2\cos(\theta_s)$; and
Type III: $\cos(\theta_s) < e < 1 + 2\cos(\theta_s)$.

Representative examples of these solutions in the phase portrait of the equations of motion (3.1) are shown in figure 5*b*. Apart from initial conditions that lie on W^s, the trajectories (θ, θ') all exit the region $\mathcal{R}$ in a finite period of time. Thus, rolling motions do not persist.

(b) The possibility of jumping

Loss of contact is a necessary, but not sufficient, condition for jumping to occur. For jumping to occur, we require that $N \searrow 0$ and that $\dot{\tilde{y}} > 0$ at the instant when the normal force vanishes.

[9] As anticipated because $I = 0$, the resultant moment of this pair of forces about m_2 vanishes.

However,

$$\dot{\hat{y}} = -R\dot{\theta}\sin(\theta) \quad \text{and} \quad \hat{\dot{y}}' = -\theta' \sin(\theta). \tag{3.11}$$

After examining the phase portraits shown in figures 4 and 5*b*, we conclude that when $N \searrow 0$, $\theta' \sin(\theta) > 0$ and thus, $\dot{\hat{y}} < 0$. Hence, spontaneous jumping without prior slipping for this rigid body does not occur. That is, the Type I and Type II motions do not lead to jumping. If jumping is possible, then it must occur for Type III motions. However, these motions of the rigid body exhibit slipping while $N > 0$. Thus, to establish any conclusions for the motions, we need to examine the equations of motion for the sliding rigid body.

Turning to Littlewood's comments about the rolling hoop, we recall that he stated that the hoop would jump when $\theta = \pm(\pi/2)$. For θ to reach this value, we note from the static friction criterion (cf. (3.9)) that $\mu_s > 1$. However, even if $\mu_s > 1$, our analysis shows that $\dot{\hat{y}} < 0$ when N vanishes and so jumping cannot occur. Littlewood also points out that he expects the hoop to slide before jumping. We now turn to examining the interesting dynamics of the sliding rigid body.

(c) Gliding motions

The governing dimensionless equations of motion for the sliding rigid body are found by simplifying (2.16) and employing the dimensionless time variable τ:

$$\hat{\mathbf{M}} \begin{bmatrix} \eta'' \\ \theta'' \end{bmatrix} + \begin{bmatrix} \sin(\theta)\,\theta'\theta' \\ -\sin(\theta)\,\theta'\theta' \end{bmatrix} = \begin{bmatrix} -\mu_k \hat{N} s \\ \sin(\theta) \end{bmatrix}, \tag{3.12}$$

where $s = (\eta'/|\eta'|)$ is the slip direction and the dimensionless mass matrix $\hat{\mathbf{M}}$ is

$$\hat{\mathbf{M}} = \begin{bmatrix} 1 & -1 - \cos(\theta) \\ -\cos(\theta) - 1 & 2(1 + \cos(\theta)) \end{bmatrix}. \tag{3.13}$$

The dimensionless normal force is given by

$$\hat{N} = \frac{N}{m_2 g} = 1 - \left(\sin(\theta)\,\theta'' + \cos(\theta)\,\theta'\theta'\right). \tag{3.14}$$

To integrate (3.12), we need to introduce the expression for $\hat{N}$ and then derive a set of differential equations for θ and η. The mass matrix $\hat{M}$ associated with the kinetic energy for the sliding body is non-invertible when $\theta = 0, \pm\pi$. Consequently, we anticipate issues when attempting to analyse the equilibrium configuration where $\theta = 0$ and $\theta = \pm\pi$. For future reference, we note that $\hat{N} = 1$ for these configurations.

After inverting $\hat{M}$ and solving for η'' and θ'', we find the pair of equations

$$\begin{aligned} \eta'' &= \frac{1}{1 - \cos(\theta)} \left(\sin(\theta)\left(1 - \theta'\theta'\right) - 2\mu_k \hat{N} s\right), \\ \theta'' &= -\frac{1}{\sin(\theta)} \left(-1 + \cos(\theta)\,\theta'\theta' + \mu_k \left(\cot(\theta) + \operatorname{cosec}(\theta)\right) \hat{N} s\right). \end{aligned} \tag{3.15}$$

With the help of (3.14), we remarkably find that $(3.15)_2$ reduces to an equation for $\hat{N}$:

$$\hat{N}\left(1 - \mu_k s \left(\cot(\theta) + \operatorname{cosec}(\theta)\right)\right) = 0. \tag{3.16}$$

Thus, solutions to the equations of motion (3.12) are possible only when $\hat{N} = 0$. In this case the body is said to be gliding on the ground plane. Because there is no friction force, the energy of the rigid body is constant during this motion. In 1997, Tokieda [12] was the first to observe that gliding motions occur. The first detailed analysis of these motions was published four years later by Theron and du Plessis [17].

An alternative method to establish that N must vanish is to consider the moment balance: $I\ddot{\theta} = (\boldsymbol{\pi}_{\mathrm{P}} \times (\mathbf{F}_f + \mathbf{N})) \cdot \mathbf{E}_3$. For the system of interest, $I = 0$ and $\mathbf{F}_f$ is an assumed linear function of N. It is then straightforward to show that $\mathbf{N}$ and, consequently, $\mathbf{F}_f$ must vanish. This conclusion also applies for the more general case where the particle is not located on the rim: $\ell \in (0, R)$. We define

a motion of a rigid body on a surface with a vanishing normal force as a gliding motion. For such motions, the balance of linear momentum for the rigid body can then be used to conclude that the trajectory of the centre of mass (i.e. the particle of mass m_2) is either a parabola or a straight vertical line.

We take this opportunity to note that Littlewood's hoop is not the only problem in the dynamics of rigid bodies where a constraint forces or moment vanishes even when the constraint is satisfied. For instance, consider a pendulum in motion on a vertical plane. It is easy to show that the normal force exerted by the plane on the pendulum vanishes (cf. [23, Section 2.4]). A second example is a rigid body dynamics model for the eye where the rigid body is subject to Listing's constraint. It can be shown that the constraint moment needed to enforce the constraint vanishes for certain motions (cf. [25,26]). As with a rolling or gliding Littlewood's hoop, the balance laws, constraints and prescriptions for the constraint forces and constraint moments for these problems provide a determinate system of equations to determine the motion of the system that satisfies the constraints and the constraint forces and constraint moments.

The equations of motion for the rigid body when $\hat{N} = 0$ can be determined from (3.12) by setting $\hat{N} = 0$:

$$\sin(\theta)\,\theta'' + \cos(\theta)\,\theta'\theta' - 1 = 0 \quad \text{and} \quad \eta'' = \frac{(1 - \theta'\theta')\sin(\theta)}{1 - \cos(\theta)}. \tag{3.17}$$

This pair of differential equations correspond to the respective $\mathbf{E}_2$ and $\mathbf{E}_1 - \mathbf{e}_1$ components of the balance of linear momentum $\mathbf{F} = m\bar{\mathbf{a}}$ where $\mathbf{F} = -mg\mathbf{E}_2$. As discussed earlier, the balance of angular momentum has been used to show that $\mathbf{N}$ and, consequently, $\mathbf{F}_f$ vanishes. As anticipated from our earlier remarks, the differential equations (3.17) are not defined when $\theta = 0, \pm\pi$. The differential equation $(3.17)_1$ for θ has a first integral $w = w(\theta, \theta')$ and the equations of motion (3.17) conserve the total energy $e_s = e_s(\theta, \theta', \eta')$ and the linear momentum in the horizontal direction $v = v(\theta, \theta', \eta')$:

$$\begin{aligned} w &= \frac{1}{2}\sin(\theta)\,\theta'\theta' - \theta, \\ e_s &= (1 + \cos(\theta))\,\theta'\theta' + \cos(\theta) + \frac{1}{2}\left(\eta'\eta' - 2\eta'\theta'\,(1 + \cos(\theta))\right), \\ v &= \eta' - \theta'\,(1 + \cos(\theta))\,. \end{aligned} \tag{3.18}$$

Using the integral w, the phase portrait of $(3.17)_1$ is readily constructed (cf. figure 6*a*). From the phase portrait, we observe that the angle θ does not oscillate about $\theta = \pi$. However, concomitant with the conservation of the energy e_s, θ' becomes unbounded as $\theta \to \pm\pi$.

To determine the finite amount of time it takes for $\theta \to \pm\pi$, we exploit the fact that the sole force acting on rigid body is a gravitational force and, thus, the trajectory of m_2 will be either be a parabola or a straight vertical line. To elaborate, we denote the initial value of $(\theta(\tau), \theta'(\tau), \eta'(\tau))$ and the dimensionless time τ by $(\theta_0 = \theta(\tau_0), \theta_0' = \theta'(\tau_0), \eta_0' = \eta'(\tau_0))$ and τ_0, respectively. Then, using the dimensionless variables,

$$\begin{aligned} \hat{\hat{x}}(\tau) &= \hat{\hat{x}}_0 + \left(\eta_0' - \theta_0'\,(1 + \cos(\theta_0))\right)(\tau - \tau_0)\,, \\ \hat{\hat{y}}(\tau) &= 1 + \cos(\theta(\tau)) \\ &= 1 + \cos(\theta_0) - \theta_0' \sin(\theta_0)\,(\tau - \tau_0) - \frac{(\tau - \tau_0)^2}{2}. \end{aligned} \tag{3.19}$$

Thus, after a finite interval of time $\tau_g - \tau_0$, $\hat{\hat{y}}(\tau_1) = 0$ and $\theta(\tau_g) = \pi$:

$$\tau_g - \tau_0 = -\theta_0' \sin(\theta_0) \pm \sqrt{\theta_0'\theta_0' \sin^2(\theta_0) + 2\,(1 + \cos(\theta_0))}. \tag{3.20}$$

When the initial conditions for the motion are such that $\eta_0' - \theta_0'(1 + \cos(\theta_0)) = 0$, the path of m_2 will be a vertical line.

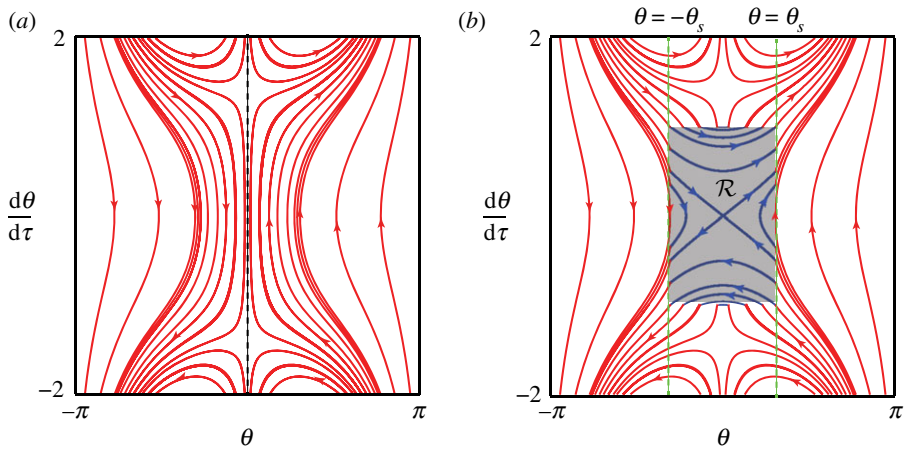

Figure 6. (*a*) Phase portrait of the equation of motion $(3.17)_1$ for $\theta(t)$ for the gliding rigid body. (*b*) Combined phase portrait for the rigid body assuming transitions to and from rolling. The shaded region corresponds to the region $\mathcal{R}$ of state space for the rolling rigid body. For the results shown in the figure, $\mu_s = 0.5$. (Online version in colour.)

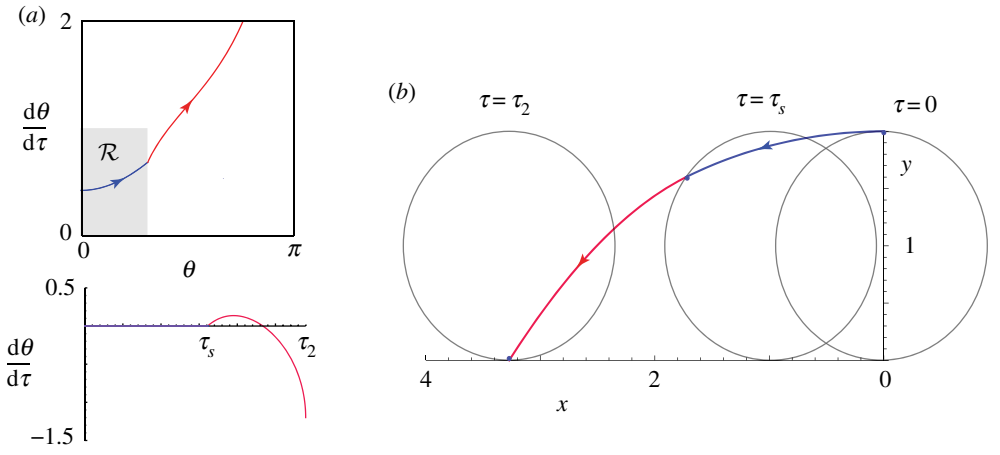

Figure 7. (*a*) Phase portrait of a motion that initially rolls and then glides along with the corresponding time trace of $\eta'(\tau)$. (*b*) The corresponding path of the mass particle m_2 during the rolling (blue) and gliding (red) phases of motion. As $\tau \to \tau_g$, $\theta \to \pi$. For the solution shown in this figure, $\theta(0) = 0$, $\theta'(0) = 0.5$, $\mu_s = 0.5$, $\tau_s \approx 1.6094$ and $\tau_g \approx \tau_s + 1.2868$. An animation of the results shown in (*b*) can be found in the electronic supplementary material data. (Online version in colour.)

(d) Transitions from rolling to gliding

The dynamics of the rigid body can be analysed by composing a dynamical system as follows. We suppose that an initial condition starts in the region $\mathcal{R}$ defined previously. Thus, the dynamics of the rolling rigid body are governed by (3.1). At time $\tau = \tau_s$, the trajectory exits $\mathcal{R}$, a transition to gliding occurs. At the instant where gliding starts, $\eta' = 0$, $\theta(\tau)$ is governed by $(3.12)_1$, and $\eta(t)$ is governed by $(3.17)_2$. From our earlier remarks, we can conclude that $\theta \to \pi$ in a finite time $\tau_g - \tau_s$ (cf. (3.20)). These dynamics are summarized in the phase portrait shown in figure 6*b* and an example of the motions described here is shown in figure 7. From this figure, we note that the path of m_2 during rolling is a cycloid and the path is a parabola when the rigid body is gliding. We also note from the time trace of $\eta'(\tau)$ for this example that, even though η' vanishes for an instant, there is insufficient static friction to maintain rolling and gliding persists.

(e) Transitions to and from gliding

The dynamics of the gliding body can be understood by examining the trajectory $(\theta(\tau), \theta'(\tau), \eta'(\tau))$ in a three-dimensional state space $\mathcal{S}$. In order for the body to transition from gliding to rolling, we need $\eta'(\tau) = 0$ when $(\theta(\tau), \theta'(\tau)) \in \mathcal{R}$. Thus, the trajectory needs to intersect the region $\mathcal{R}$ on the plane $\eta' = 0$ in the state space $\mathcal{S}$. When this happens, the body transitions from gliding to rolling. Referring to figure 6*b*, we observe that, apart from the case where the intersection lies on the stable manifold to the equilibrium point $(\theta = 0, \theta' = 0)$, all of the trajectories on $\mathcal{R}$ exit this region and the body will start gliding. If the trajectory does not intersect $\mathcal{R}$, then gliding persists and $\theta \to \pm\pi$ in finite time.

4. Conclusion

We have explored the dynamics of the simplest known example of a single rigid body that exhibits self-induced jumping. While this behaviour was first mentioned by Littlewood, an analysis of his model leads to paradoxical behaviour of a body that can roll but cannot support the normal force needed to slide and cannot jump. As can be appreciated by comparing the phase portraits shown in figures 2*b* and 4 and 6, by incorporating the inertia of the rigid body, we find a dramatically different dynamical system describing the motion of the rigid body. In particular, we confirm the self-induced jumping and transitions from rolling to sliding motions observed by others. The self-induced jumping exhibited by the rigid body is the simplest example of this phenomenon in classical mechanics.

Data accessibility. Electronic supplementary material, videos for figures 3 and 7 are included in this paper. A third video shows a motion of the rolling rigid body where the body oscillates about its stable equilibrium configuration.

Authors' contributions. Both authors participated equally in the development of the models, numerical analyses and analysis of the data and devising the structure of the paper. The corresponding author, O.O., was primarily responsible for writing the final manuscript and A.B. developed the animations of the rigid body. Both authors gave final approval for publication and agree to be held accountable for the work performed therein.

Competing interests. The authors declare no competing interests.

Funding. This research was not supported by external funds.

Acknowledgements. The authors wish to thank Prof. Alexander P. Ivanov for providing copies of [21,22] and to Dr Bair Budaev for his invaluable help translating [22]. O.M.O. is grateful to the late Hans Wolfgang Liepmann for introducing him to [11]. While an earlier draft of this paper was under review, Prof. Andy Ruina (Cornell University) kindly pointed the authors to the papers [13,15,17–20] on Littlewood's hoop that were inspired by Tokieda's analysis in [12].

References

1. Batista M. 2008 Self-induced jumping of a rigid body of revolution on a smooth horizontal surface. *Int. J. Non-Linear Mech.* **43**, 26–35. (doi:10.1016/j.ijnonlinmec.2007.09.010)
2. Ivanov AP. 2008 On detachment conditions in the problem on the motion of a rigid body on a rough plane. *Regul. Chaotic Dyn.* **13**, 355–368. (doi:10.1134/S1560354708040096)
3. Mitsui T, Aihara K, Terayama C, Kobayashi H, Shimomura Y. 2006 Can a spinning egg really jump? *Proc. R. Soc. A* **462**, 2897–2905. (doi:10.1098/rspa.2006.1718)
4. Schiehlen W, Gao J. 1989 Simulation des stoßfreien Hüpfen. *Z. Angew. Math. Mech.* **69**, T302–T303.
5. Shimomura Y, Branicki M, Moffatt HK. 2005 Dynamics of an axisymmetric body spinning on a horizontal surface. II. Self-induced jumping. *Proc. R. Soc. A* **461**, 1753–1774. (doi:10.1098/rspa.2004.1429)
6. Blackowiak AD, Rand RH, Kaplan H. 1997 The dynamics of the celt with second-order averaging and computer algebra. In *Proc. of DETC'97: 1997 ASME Design Engineering Technical Conferences, Sacramento, CA, 14–17 September*. Paper Number DETC97/VIB–4103. New York, NY: ASME.

7. Routh EJ. 1905a *The elementary part of a treatise on the dynamics of a system of rigid bodies*, 7th edn. London, UK: Macmillan.
8. Routh EJ. 1905b *The advanced part of a treatise on the dynamics of a system of rigid bodies*, 6th edn. London, UK: Macmillan.
9. Kessler P, O'Reilly OM. 2002 The ringing of Euler's disk. *Regul. Chaotic Dyn.* **7**, 49–60. (doi:10.1070/RD2002v007n01ABEH000195)
10. Leine RI. 2009 Experimental and theoretical investigation of the energy dissipation of a rolling disk during its final stage of motion. *Arch. Appl. Mech.* **79**, 1063–1082. (doi:10.1007/s00419-008-0278-6)
11. Littlewood JE. 1986 *Littlewood's miscellany*. Cambridge, UK: Cambridge University Press. Edited and with a foreword by Béla Bollobás.
12. Tokieda TF. 1997 The hopping hoop. *Am. Math. Mon.* **104**, 152–154. (doi:10.1080/00029890.1997.11990614)
13. Pritchett T. 1999 The hopping hoop revisited. *Am. Math. Mon.* **106**, 609–617. (doi:10.1080/00029890.1999.12005094)
14. Maritz MF, Theron WFD. 2012 Experimental verification of the motion of a loaded hoop. *Am. J. Phys.* **80**, 594–598. (doi:10.1119/1.3697837)
15. Taylor A, Fehrs M. 2010 The dynamics of an eccentrically loaded hoop. *Am. J. Phys.* **78**, 496–498. (doi:10.1119/1.3300613)
16. Butler JP. 1999 Hopping hoops don't hop. *Am. Math. Mon.* **106**, 565–568. (doi:10.1080/00029890.1999.12005084)
17. Theron WFD, du Plessis NM. 2001 The dynamics of a massless hoop. *Am. J. Phys.* **69**, 354–359. (doi:10.1119/1.1313521)
18. Lubarda VA. 2009 Dynamics of a light hoop with an attached heavy disk: inside an interaction pulse. *J. Mech. Mater. Struct.* **4**, 1027–1040. (doi:10.2140/jomms.2009.4.1027)
19. Theron W, Maritz M. 2008 The amazing variety of motions of a loaded hoop. *Math. Comput. Model.* **47**, 1077–1088. (doi:10.1016/j.mcm.2007.06.031)
20. Yanzhu L, Yun X. 2004 Qualitative analysis of a rolling hoop with mass unbalance. *Acta Mech. Sin.* **20**, 672–675. (doi:10.1007/BF02485872)
21. Ivanov AP. 1993 On shock-free jump of a non-homogeneous wheel: 1. Smooth supporting surface. *Izvestiya Rossiiskoi Akademii Nauk, Seriya Mechanika Tverdogo Tela*, pp. 25–31. In Russian. (doi:10.31857/s2587-556620191)
22. Ivanov AP. 1993 On shock-free jump of a non-homogeneous wheel: 2. Rough supporting surface. *Izvestiya Rossiiskoi Akademii Nauk, Seriya Mechanika Tverdogo Tela*, pp. 61–64. In Russian. (doi:10.31857/s2587-556620191)
23. O'Reilly OM. 2019 *Engineering dynamics: a primer*, 3rd edn. Cham, Switzerland: Springer Nature.
24. Hemingway EG, O'Reilly OM. 2018 Perspectives on Euler angle singularities, gimbal lock, and the orthogonality of applied forces and applied moments. *Multibody Sys. Dyn.* **44**, 31–56. (doi:10.1007/s11044-018-9620-0)
25. Cannata G, Maggiali M. 2008 Models for the design of bioinspired robot eyes. *IEEE Trans. Rob.* **24**, 27–44. (doi:10.1109/TRO.2007.906270)
26. Novelia A, O'Reilly OM. 2015 On the dynamics of the eye: geodesics on a configuration manifold, motions of the gaze direction and Helmholtz's theorem. *Nonlinear Dyn.* **80**, 1303–1327. (doi:10.1007/s11071-015-1945-0)